

Supporting Materials

From Amorphous to Crystalline: A Universal Strategy for Structure Regulation of High-Entropy Transition Metal Oxides

Dawei Lai,^{1†} Li Ling,^{1†} Mengfei Su,² Qiaoling Kang,² Feng Gao,^{1,*} Qingyi Lu^{2,*}

¹ Department of Materials Science and Engineering, Jiangsu Key Laboratory of Artificial Functional Materials, Collaborative Innovation Center of Advanced Microstructures, College of Engineering and Applied Sciences, Nanjing University, Nanjing 210023, P. R. China. E-mail: fgao@nju.edu.cn

² State Key Laboratory of Coordination Chemistry, Coordination Chemistry Institute, Collaborative Innovation Center of Advanced Microstructures, School of Chemistry and Chemical Engineering, Nanjing University, Nanjing 210023, P. R. China. E-mail: qylu@nju.edu.cn

† These authors contributed equally to the work.

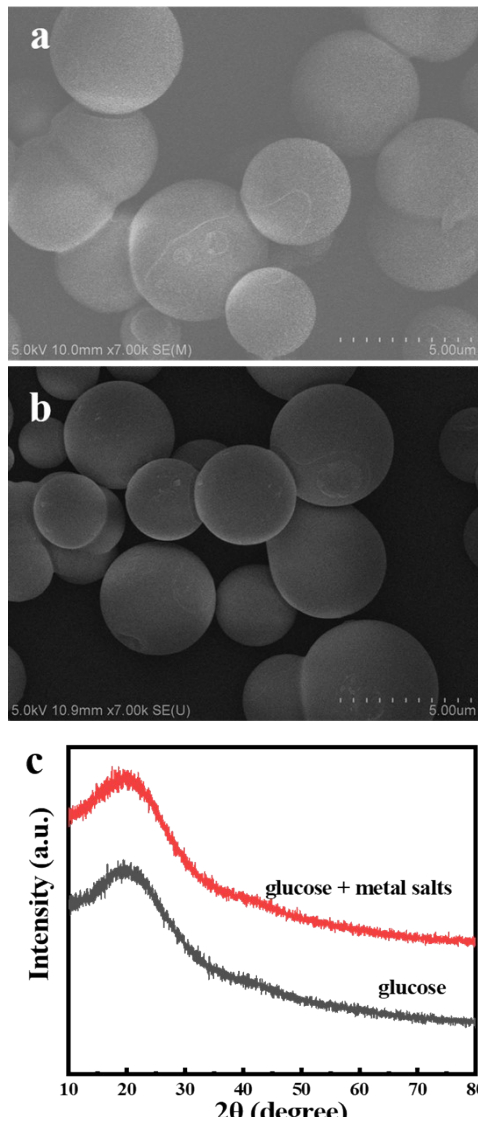


Figure S1 (a) SEM image of carbon spheres prepared without the addition of metal sources; (b) SEM image of the CrMnFeCoNi@C precursor; (c) XRD patterns of the carbon spheres and the CrMnFeCoNi@C precursor.

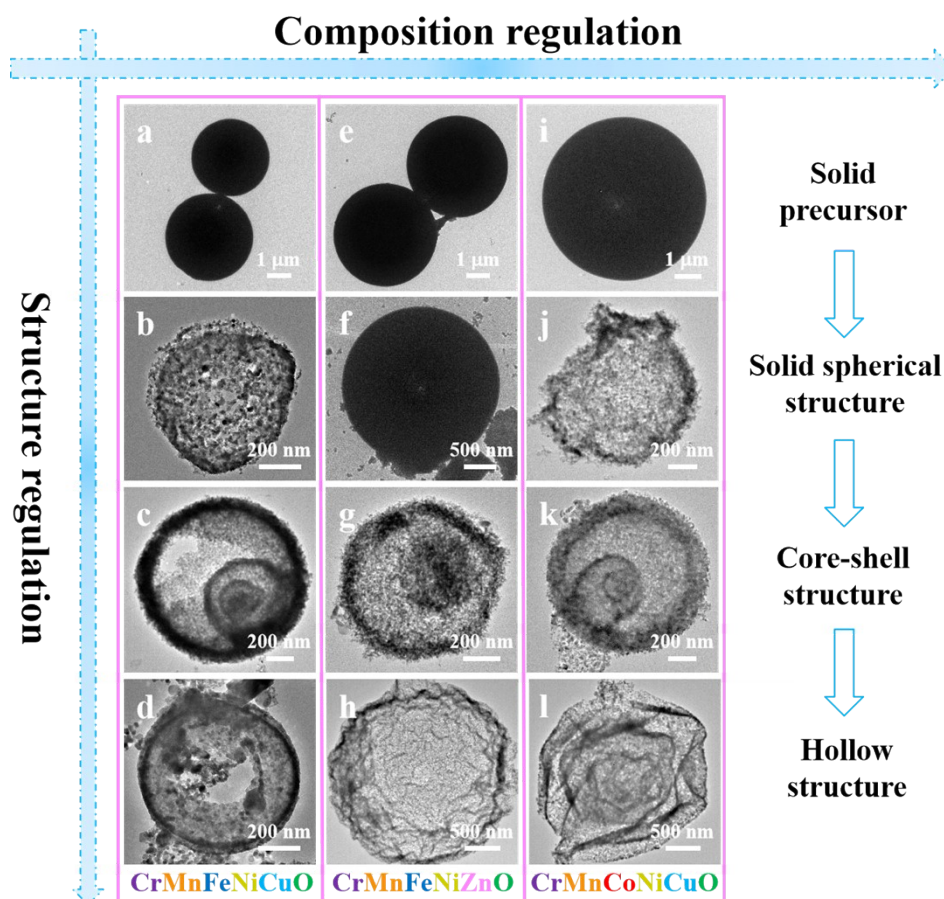


Figure S2 The structural evolution of HEMOs demonstrated by TEM images: (a~d) Cr-Mn-Fe-Ni-Cu; (e~h) Cr-Mn-Fe-Ni-Zn and (i~l) Cr-Mn-Co-Ni-Cu.

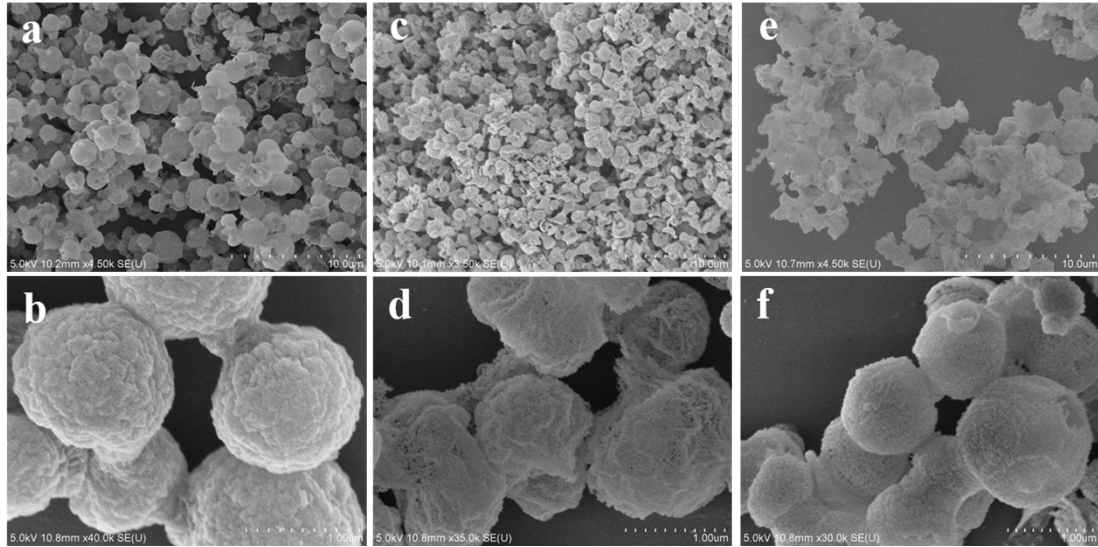


Figure S3 SEM images of (a,b) s-CrMnFeCoNiO; (c,d) c-CrMnFeCoNiO and (e,f) h-CrMnFeCoNiO.

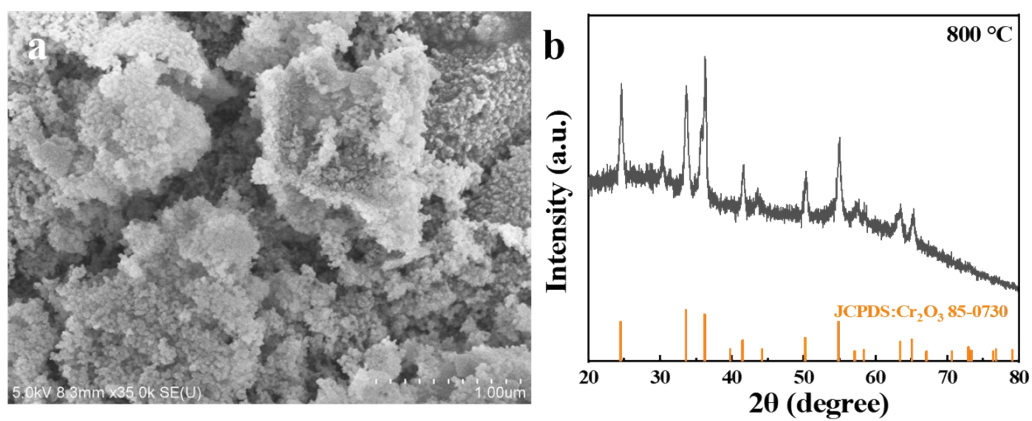


Figure S4 (a) SEM image and (b) XRD pattern of the sample prepared by calcining the amorphous precursor at 800 °C.

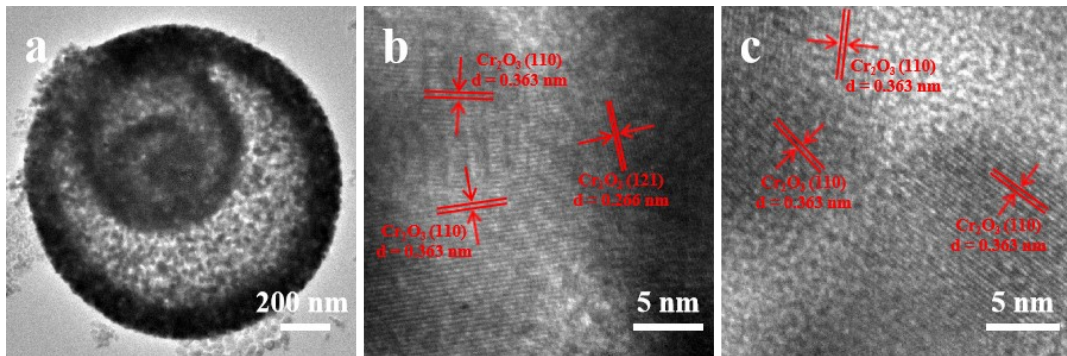


Figure S5 (a) TEM and (b, c) HRTEM images of c-CrMnFeCoNiO.

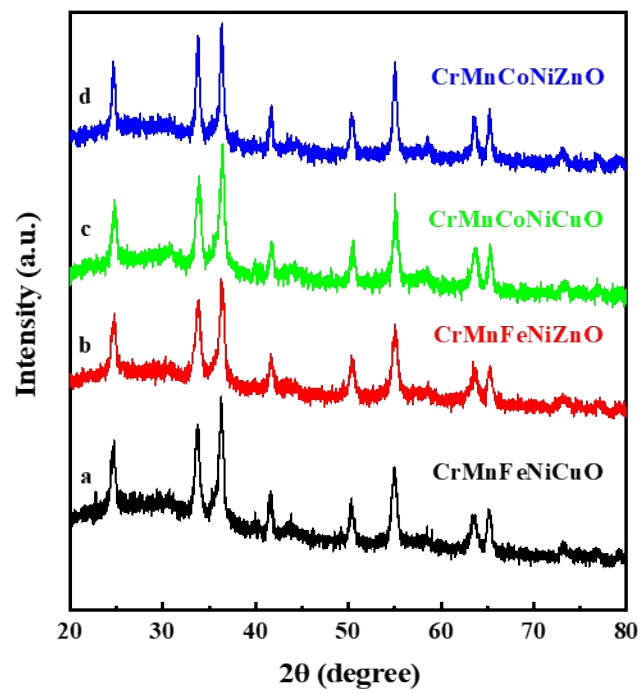


Figure S6 XRD patterns of the high entropy metallic oxides with different metal species: (a) CrMnFeNiCuO ; (b) CrMnFeNiZnO ; (c) CrMnCoNiCuO and (d) CrMnCoNiZnO .

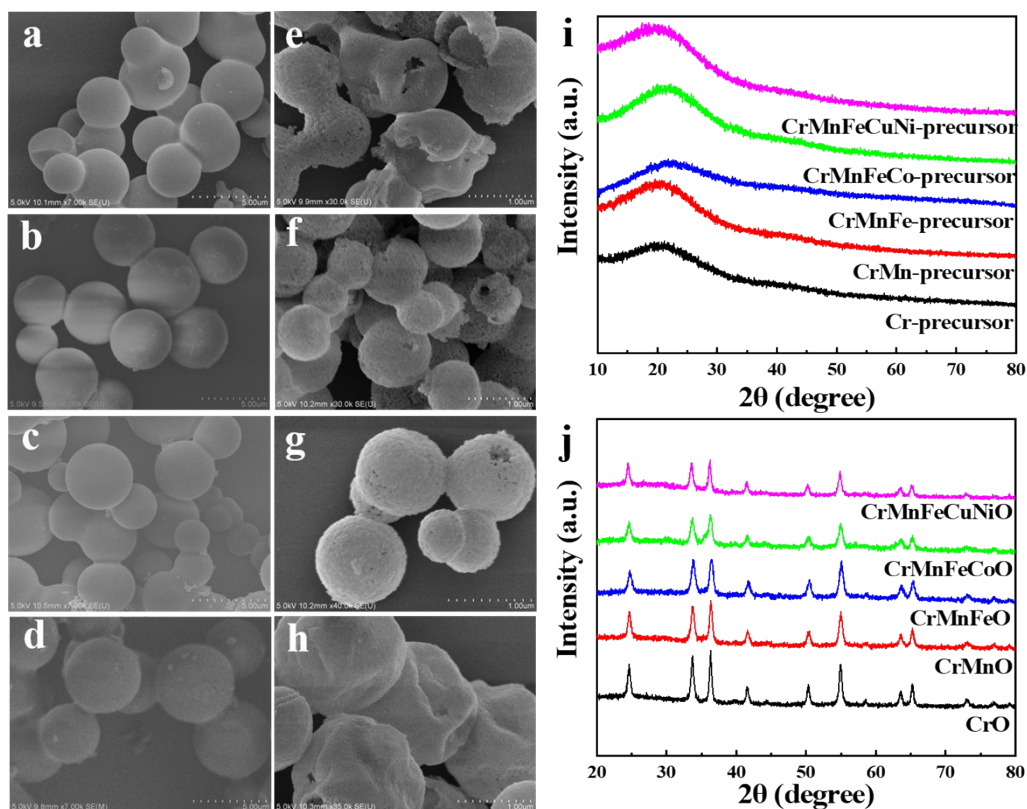


Figure S7 (a~d) SEM images of the amorphous precursors with (a) Cr; (b) CrMn; (c) CrMnFe and (d) CrMnFeCo; (e~h) SEM images of the crystalline oxides: (e) CrO; (f) CrMnO; (g) CrMnFeO and (h) CrMnFeCoO; and (i) XRD patterns of the amorphous precursors and (j) XRD patterns of of the crystalline oxides.

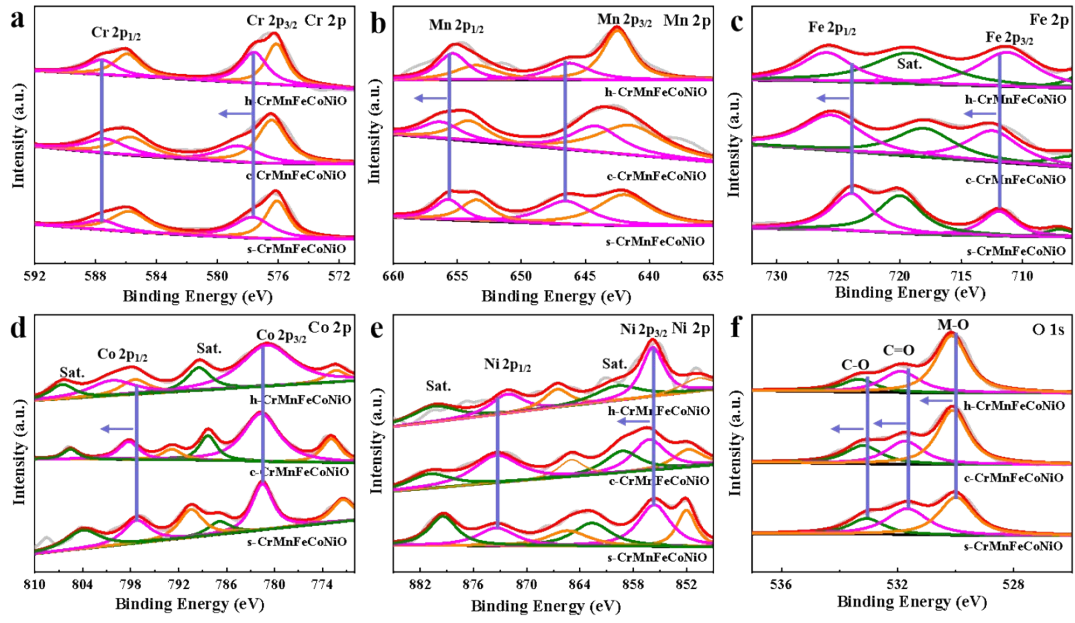


Figure S8 High resolution XPS spectra of (a) Cr 2p; (b) Mn 2p; (c) Fe 2p; (d) Co 2p; (e) Ni 2p and (f) O 1s of s-CrMnFeCoNiO, c-CrMnFeCoNiO and h-CrMnFeCoNiO.

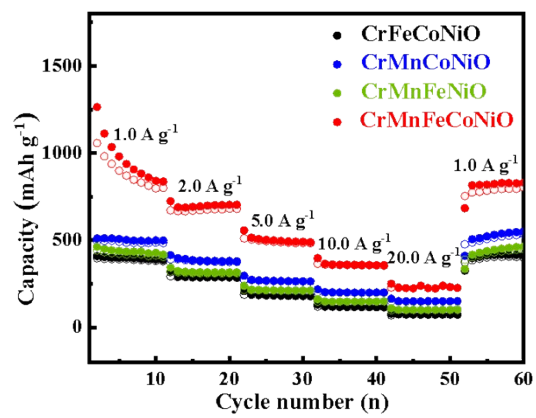


Figure S9 Rate capability of c-CrFeCoNiO, c-CrMnCoNiO, c-CrMnFeNiO and c-CrMnFeCoNiO.

Table S1 The LIBs performance comparisons of the core-shell CrMnFeCoNiO spheres with recently-reported LIBs anodes.

Materials	Specific Capacity	Reference
c-CrMnFeCoNiO	753 mAh g⁻¹ @ 1.0 A g⁻¹ 960 mAh g⁻¹ @ 0.5 A g⁻¹	This work
MS ₂	812 mAh g ⁻¹ @ 0.5 A g ⁻¹	<i>Adv. Energy Mater.</i>
MS	595 mAh g ⁻¹ @ 1.0 A g ⁻¹	2022 , 12, 2103090
(CrNiMnFeCu) ₃ O ₄	556 mAh g ⁻¹ @ 1.0 A g ⁻¹ 647 mAh g ⁻¹ @ 0.5 A g ⁻¹	<i>Adv. Funct. Mater.</i> 2022 , 32, 202110992
CNT-on-OCNT-Fe	560 mAh g ⁻¹ @ 1.0 A g ⁻¹	<i>Adv. Funct. Mater.</i> 2018 , 28, 1801746
(Co _{0.2} Cr _{0.2} Fe _{0.2} Mn _{0.2} Ni _{0.2}) ₃ O ₄	555 mAh g ⁻¹ @ 0.2 A g ⁻¹	<i>Nat. Commun.</i> 2018 , 9, 3400
MnO@NC	570 mAh g ⁻¹ @ 1.0 A g ⁻¹	<i>Adv. Funct. Mater.</i> 2018 , 28, 1800003
VEG at 60 °C	550 mAh g ⁻¹ @ 1.0 A g ⁻¹	<i>Adv. Energy Mater.</i> 2018 , 8, 1801978
b-MnO ₂ ALAT	520 mAh g ⁻¹ @ 1.0 A g ⁻¹	<i>Adv. Mater.</i> 2020 , 32, 1906582
Mg _{0.2} Co _{0.2} Ni _{0.2} Cu _{0.2} Zn _{0.2} O	600 mAh g ⁻¹ @ 0.089 A g ⁻¹	<i>Energy Environ. Sci.</i> 2021 , 14, 2883
Cu-HHTQ	600 mAh g ⁻¹ @ 0.6 A g ⁻¹	<i>Angew. Chem. Int. Ed.</i> 2021 , 60, 24467
Li ₂ GeO ₃	725 mAh g ⁻¹ @ 0.05 A g ⁻¹	<i>Angew. Chem. Int. Ed.</i> 2016 , 55, 16059
LLTO	449 mAh g ⁻¹ @ 0.2 A g ⁻¹	<i>Nat. Commun.</i> 2020 , 11, 3490